RSC Advances

PAPER

View Article Online
View Journal | View Issue

Cite this: *RSC Adv.*, 2015, **5**, 35311

A novel thermal reflow method for the fabrication of microlenses with an ultrahigh focal number

M. Wang,[ab] W. Yu,*[c] T. Wang,[a] X. Han,[a] Erdan Gu*[d] and X. Li[e]

In this paper, we demonstrate a novel thermal reflow method with an additional near ultraviolet (UV) flood exposure and upside-down reflow configuration for the fabrication of microlenses with an ultrahigh focal number. By using this method, microlenses with a focal number ($F^{\#}$) as high as 9.7 have been successfully obtained, which is about four fold higher than that can be fabricated with a conventional reflow method. The final profile of the microlenses can be flexibly and accurately tuned by controlling the flood exposure dosage and adopting the appropriate reflow configuration, which enables fabrication not only of spherical microlenses but also of more complex aspheric lenses. The fabricated microlens is characterized by measuring the point spread function (PSF) and the measurement result indicates that the diffraction limited optical performance of the microlens can be achieved. The method developed in this work can be used for the mass and cost-effective fabrication of high performance microlenses with ultrahigh focal numbers, which can find applications such as in accurate optical testing, integration imaging, and laser beam collimating.

Received 16th January 2015
Accepted 13th April 2015

DOI: 10.1039/c5ra00957j

www.rsc.org/advances

Introduction

The refractive microlens is a versatile photonic element gaining everlasting interest for various applications.[1–8] The geometry of the microlens will be different for different application purposes. For instance, microlenses with a larger focal number ($F^{\#}$), corresponding to a lower numerical aperture (NA), are preferred in order to improve the detecting accuracy of Hartmann–Shack wave front sensors.[9] So far, a lot of methods have been developed to fabricate microlenses for various applications, among which the thermal reflow method stands out for its simplicity, excellent lens uniformity and good compatibility with the well-established IC manufacturing flow and therefore is mass productive yet cost-effective.[1,10–20,22] This method takes advantage of the surface tension of the molten photoresist so that a spherical surface profile can be formed to retain the minimum surface energy state when the photoresist cylinder is heated above its glass transition temperature (T_g).[1,11]

Generally speaking, conventional thermal reflow yields microlens with $F^{\#}$ ranging from 0.8 to 2 (or in NA, 0.6 to 0.25).[12] It seems problematic to fabricate larger $F^{\#}$ microlenses for a dip will turn up in the center of the molten resist pattern when its diameter increases.[11,13] The origin of the dip could be attributed to the constraint of the contact angle,[11,13] the inadequate photoresist volume,[13] the inappropriate reflow temperature setting,[14] or the crosslinking nature of photoresist polymers.[15,16] To further increase the $F^{\#}$ of the fabricated microlens, various methods have been proposed and demonstrated. S. Haselbeck *et al.* introduced a resist base layer to reduce the contact angle so that the microlens with a NA as low as 0.1 can be fabricated.[13] Another feasible approach is to use the laser direct writing method to fabricate microlenses with expected focal number in photoresist first and then followed by a thermal reflow to further increase the smoothness of the surface.[17] By using this method, $F^{\#}$ can be increased to 4.5.[17] Insufficient exposure and development of photoresist, which can form a residual photoresist layer naturally after development, are proved effective to improve $F^{\#}$ to about 10.[18–20] However, this method may face trade-off between lens profile accuracy and fill factor for photoresist may reflow all over the substrate without strong boundary constraint. Efforts are still needed to explore new approaches with shorter process cycle yet less complexity and less cost to fabricate microlenses with high $F^{\#}$ and controllable surface profile.

Methods and experimentals

In this paper, we demonstrate a novel thermal reflow method which can increase the $F^{\#}$ of the fabricated microlens by more

[a]*State Key Laboratory of Applied Optics, Changchun Institute of Optics, Fine Mechanics & Physics, Chinese Academy of Sciences, No. 3888, Dongnanhu Road, Changchun, Jilin, P. R. China*

[b]*University of Chinese Academy of Sciences, Beijing, 100049, P. R. China*

[c]*Institute of Micro & Nano Optics, Key Laboratory of Optoelectronic Devices and Systems of Ministry of Education, College of Optoelectronic Engineering, Shenzhen University, Shenzhen, 518060, Guangdong Province, P. R. China. E-mail: yuwx@szu.edu.cn*

[d]*Institute of Photonics, University of Strathclyde, Glasgow G4 0NW, UK. E-mail: erdan.gu@strath.ac.uk*

[e]*Quality Test Center, Changchun Institute of Optics, Fine Mechanics & Physics, Chinese Academy of Sciences, No. 3888, Dongnanhu Road, Changchun, Jilin, P. R. China*

than 4.5 times in comparison with the microlens made by a conventional thermal reflow method. Besides, this method is easy to be applied for mass and cost-effective fabrication and the accurately. In this approach, two significant modifications have been made based on the normal thermal reflow method. One is that an additional UV flood exposure of the photoresist cylinders after development and before thermal reflow is added. We utilize an I-line (365 nm) UV lamp as the flood exposure source as the positive photoresist patterns cured by such near UV light are easier to reflow while deep UV irradiation has a negative effect.[21] In addition, near UV flood exposure can lower the T_g of the photoresist.[10] Considering the positive correlation between thermal-crosslinking rate and temperature,[15] this is advantageous because the molten photoresist has relatively more chance to approach the ideal spherical shape before it is thoroughly crosslinked. The other modification is to implement the thermal reflow with an upside-down configuration, that is to say the substrate is flipped with photoresist facing the hotplate but not the backside of the substrate. This is to take advantage of the gravity. The gravity effect is usually negligible and ignored when dealing with microlenses with a small curvature radius,[22] however, it can be remarkable for high $F^{\#}$ microlenses that have a larger curvature radius. This can be illustrated in terms of Bond number ($B_o \equiv \rho g R^2/\sigma$), which is widely used in fluidics to weigh the relative effect of gravity and surface tension that impose on a droplet.[23] Here, ρ, g, R and σ denote mass density, gravitational acceleration, curvature radius and surface tension of photoresist, respectively. Then we can see B_o increases with curvature radius quadratically. By replacing R with $F^{\#}$ and base diameter (D), a more illustrating form of B_o is obtained: $B_o = \rho g[(n-1)DF^{\#}]^2/\sigma$, where n denotes the refractive index of the microlens. To photoresists, typical values of n, ρ and σ are about 1.6, 1000 kg m^{-3} and (2 to 5) $\times$ 10^{-2} N m^{-1}, respectively.[22] Thus for a microlens whose $F^{\#}$ and base diameter are 10 and 100 μm, the calculated B_o is around 0.1. That signifies though the surface tension dominates the reflow process, the gravity can also impose an effect on the final microlens profiles. Therefore, an upside-down reflow configuration is helpful for achieving high $F^{\#}$ microlenses because it can turn the adverse effect of gravity to a beneficial side, which has been confirmed by our results. By adding these two modifications into the conventional thermal reflow process, it is found that the $F^{\#}$ of the fabricated microlens can be increased significantly. It is also found this method has the potential to produce microlenses with a controllable profile. Moreover, this technique is of good compatibility with other available fabrication methods and therefore an even higher $F^{\#}$ microlens is possible to be fabricated through a smart combination of these methods.

Fig. 1 depicts the modified thermal reflow process where standard photolithography is firstly conducted to obtain photoresist cylinder array followed by flood exposure and then thermal reflow with upside-down configuration. As the volume and base diameter of a photoresist cylinder only change slightly during thermal reflow, one can tune the dimensions of initial resist cylinders to produce desired $F^{\#}$ microlenses. In our experiments, the height and base diameter of photoresist cylinders are controlled by adjusting spin-coating speed and selecting binary glass/chromium photomasks with different size of patterns, respectively. The detail of the process flow is as follows: firstly, a positive photoresist (Shipley 1813, Shipley) was spun coated on a cleaned bare silicon wafer at a variety of speeds ranging from 800 rpm to 4000 rpm to obtain photoresist layers with different thicknesses ranging from 1.3 μm to 3.2 μm. Next, the samples were soft-baked on a hotplate and exposed with an I-line mask aligner. The photomask used for exposure has patterns of circle array with diameters of 45 μm and 100 μm. After full development, additional flood exposures were conducted with the same mask aligner with exposure doses of 0–4 times of that used for photolithographic patterning. Finally, samples were heated with an upside-down configuration on a hotplate with temperatures and duration set as follows: 95 °C/10 min, 115 °C/10 min, 135 °C/10 min, 155 °C/10 min, 165 °C/10 min and 180 °C/30 min. It is noted that, in our experiment, a 2 mm thick glass plate was placed in between the substrate and hotplate so that there is an open air gap in between the photoresist layer and the top surface of the hotplate. In this case, the photoresist was actually heated through the air convection but not through the intimate contact conduction, therefore a more uniform heating and reflow were obtained by this upside-down configuration. After annealing and cooled down back to room temperature, a plano-convex photoresist microlens array was successfully fabricated.

Results and discussions

Geometries of the fabricated microlenses were characterized with various methods. An optical microscope (MX61-F, Olympus) was utilized to obtain a general 2D picture. As demonstrated in Fig. 2(a), the base diameter of these microlenses is 100.39 μm, which is almost the same as that of initial photoresist cylinders. Fig. 2(b) shows the 3D image reconstructed from the measured height data by a scanning confocal microscope (OLS4000, Olympus). It should be noted that some particular height data obtained may not be accurate due to the

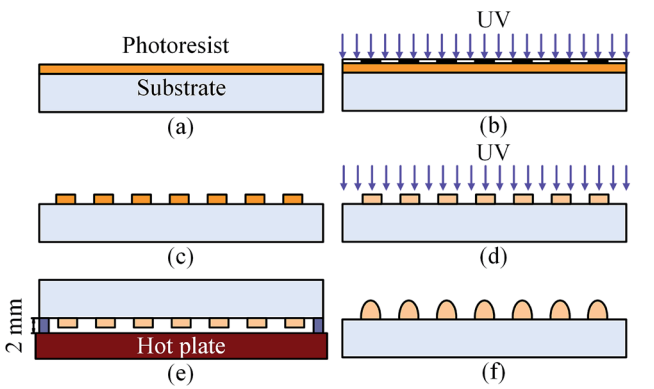

Fig. 1 Schematic of the process flow for the fabrication of high $F^{\#}$ microlens: (a) spin coating and soft bake of photoresist on a substrate, (b) UV exposure on the photoresist through a photomask, (c) photoresist cylinder array after development, (d) UV flood exposure, (e) step heating on a hotplate with upside-down configuration, (f) fabricated microlens array after annealing.

destructive interference between the lights reflected from the lenses and substrate surfaces, which results in the ripples in the 3D picture of the microlenses. Alternatively, a mechanical stylus (Alpha-Step D-100, KLA-Tencor) has been used to acquire the authentic profile, which is advisable in flat microlens case.[24] Fig. 2(c) shows the obtained microlens profile and the least square fitting to an ideal spherical shape. As is shown, the maximum profile deviation is only 0.19 μm. $F^{\#}$ of these microlenses, as calculated with the sag height and base diameter derived from the profile plot, is 9.7 (or 0.05 in NA, NA = $1/2F^{\#}$). A refractive index value of 1.6406 (at 632.8 nm) from the resist product datasheet is used in the calculation. While using a conventional method, the largest $F^{\#}$ can be obtained is only 2.4 in our experiment. This means that $F^{\#}$ of the microlens can be increased to more than 4.5 times by introducing aforementioned two modifications on the conventional thermal reflow method.

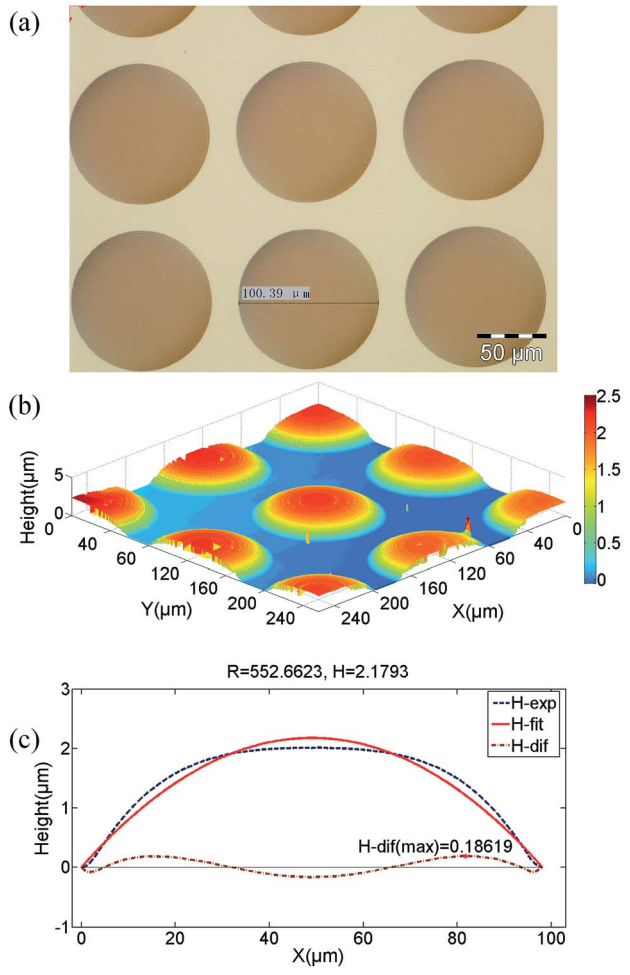

Fig. 2 Geometrical characterization results of resist microlenses formed by thermal reflowing of the photoresist cylinders with initial height 1.3 μm and base diameter 100.4 μm: (a) optical microscopy photograph, (b) reconstructed 3D image with laser scanning confocal microscope measurement data, (c) profile obtained by stylus surface profiler (blue dash line), least square fitting to an ideal spherical shape (red solid line, "*R*" and "*H*" represent its curvature radius and sag height, respectively) and the deviation between two profiles (brown dash-dot line).

To look into the separate effects of the flood exposure and the upside-down reflow configuration on the formation of microlenses, more experiments were conducted. As is demonstrated in Fig. 3, the dip in the formed photoresist microlens becomes smaller with the increase of the flood exposure dosage. We attribute this phenomenon to the complex chemical reactions of the photoresist materials with the UV light. Like many other positive photoresist, Shipley 1813 consists of novolak resin and diazo photoactive compound (PAC). The latter can be transformed to an active ketene intermediate if subjected to UV irradiation or calefaction. If there is sufficient water in the photoresist, the ketene will degrade to indene carboxylic acid. Otherwise, it will react with the novolak resin by means of ester-linkage.[25] The formation of ester-linkage, which gives rise to some degree of crosslinking, can hinder the resin from reflowing to its own limit.[26] A flood exposure with a specific dosage in ambient atmosphere before reflow is adequate to transform some portion of PAC to indene carboxylic acid and hence facilitates the reflowing process. It is found that although the flood exposure helps to reduce the dips, a spherical lens shape still cannot be formed even using a high flood exposure dosage. However, if the substrate is placed upside down during thermal reflow, the dips in all the samples disappear, indicating that the gravity plays an important role in final profile formation. In this case, the surface profile of the reflowed photoresist is still strongly influenced by the dosage of the flood exposure as shown in Fig. 3 and a spherical profile can be achieved by using high dosage flood exposure. Thus, our results demonstrate that one can accurately control the surface profile by adjusting the exposure dosage and adopting different reflow configurations.

The microlens profile change with respect to the aspect ratio (AR) of the cylinder structures was studied as well. By adjusting the spin coating speeds from 800 rpm to 4000 rpm, the ARs of the original cylinders with a diameter of 100 μm can be tuned from 0.032 to 0.013. Those cylinders were then flood-exposed

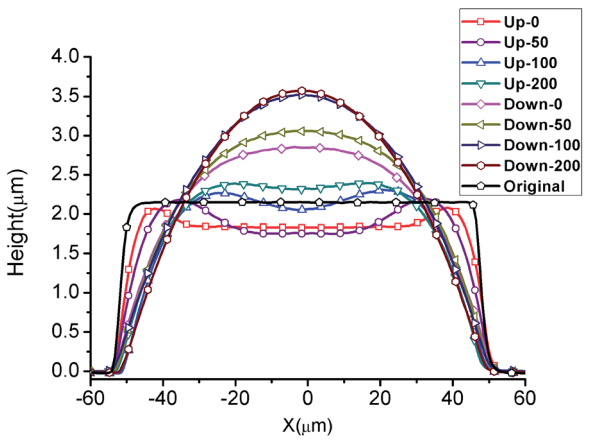

Fig. 3 Final profiles of microlenses on silicon substrate formed from resist cylinders with 100 μm diameter and 2.2 μm height. "Up" or "Down" means the substrate was placed with upside up or down, respectively. The number represents the exposure dosage, for instance, "50" means the flood exposure dosage is 50 mJ cm^{-2}, "Original" means the profile of photoresist cylinders.

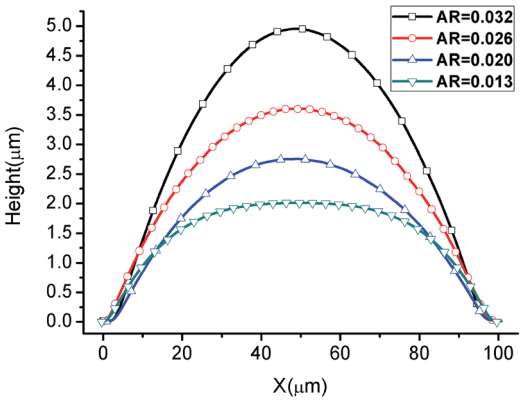

Fig. 4 Final profiles of microlenses on silicon substrate formed from resist cylinders with 100 μm diameter and various aspect ratios. The exposure dosage is 200 mJ cm^{-2} and the reflow configuration is upside-down for all cases.

with a dosage of 200 mJ cm^{-2} and placed upside down during the reflow process. Fig. 4 shows the profiles of the obtained microlenses. As is shown, the sag height of the microlens increases with the increase of the AR of the original cylinder, which means that the sag height of the formed microlens is proportional to the AR of the cylinder structures.

It is also found that the spacing between the hot plate and the inverted substrate can influence the profiles of the obtained microlens. As can be seen from Fig. 5(a)–(c), the shape of microlens changes slightly when the gap is no larger than 3 mm. However, by further increasing the gap to 5 mm and 7 mm, a flat top and a dip occurs in the center of the microlenses, which are shown in Fig. 5(d) and (e), respectively. This can be explained from two aspects. On one hand, a temperature gradient exists from the hotplate surface to the air and thus the actual temperature applied on the photoresist patterns decreases as the gap increases. On the other hand, the temperature of the hotplate in fact is set higher than the T_g of the S1813 photoresist. Therefore, if the gap is less than a certain value, the actual temperature applied on the photoresist patterns is still sufficient for them to reflow completely. In this case, the reflowed photoresist patterns will not exhibit obvious difference in shape, as shown in Fig. 5(a)–(c). Otherwise, if the gap is larger than that certain value, the photoresist patterns cannot reflow completely and thus their final shapes show notable difference as the gap increases, which is shown in Fig. 5(d) and (e).

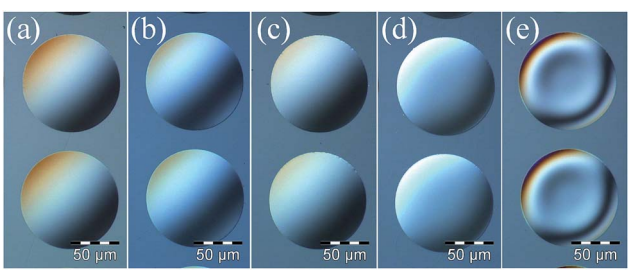

Fig. 5 Microscopic pictures of the microlens arrays fabricated with various spacings between the hot plate and the inverted substrate (1 mm, 2 mm, 3 mm, 5 mm, 7 mm, from (a) to (e), sequentially).

To verify the applicability of the method further and to characterize the optical properties of the microlenses fabricated, we used glass plate as another trial substrate. The spin-coating speed is set as 4000 rpm and the photomask is circle array with a diameter of 100 μm. Then the fabricated photoresist cylinder array was flood exposed at a dosage of 200 mJ cm^{-2}

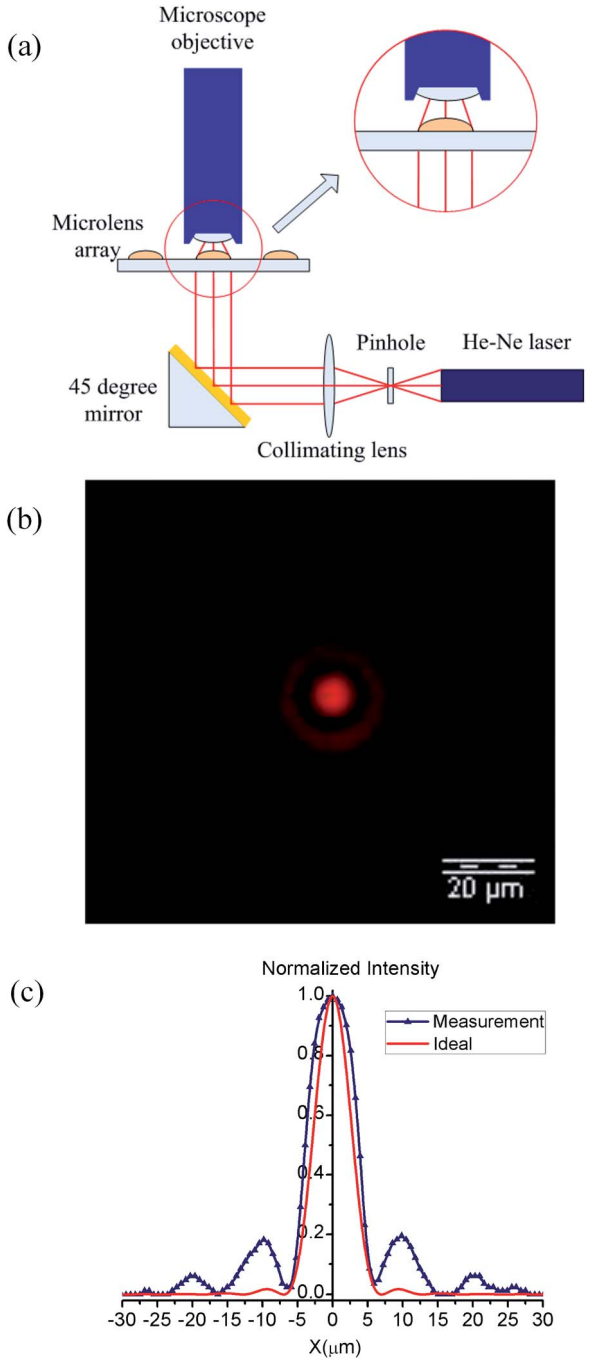

Fig. 6 Testing the PSF of the fabricated microlens with $F^{\#} = 8.9$ on glass substrate: (a) optical setup for testing the PSF, (b) captured Airy pattern of the microlens, (c) comparison between the measured PSF and the ideal diffraction-limited one.

and reflowed upside down. The same geometrical characterization and calculation method described above were used to characterize the fabricated microlens on glass substrates. The characterization results indicate that microlenses with $F^{\#}$ as high as 8.9 have been successfully fabricated. Moreover, point spread function (PSF) of the fabricated microlens is tested to characterize its optical performance with the experimental setup depicted in Fig. 6(a). In the setup, collimated He–Ne laser beam is reflected by a 45 degree-tilt mirror and incidents on the microlens array vertically. The transmission light is then collected by a 200× optical microscope. We focused the microscope at the focal plane of the microlens to capture its focal point image. Fig. 6(b) shows the captured image of the Airy pattern, in which a bright Airy disc with 13.7 μm diameter is encircled by a series of less bright concentric rings. Fig. 6(c) shows the measured 2D PSF and the ideal PSF. As can be seen, though the central peak of measured PSF is not as sharp as the ideal one, the diameters of both Airy discs are almost the same. This result indicates that a near diffraction-limited optical performance has been obtained but imperfect lens profile diffracts portion of light into higher order ring lobes. The deviation of the measured PSF from the ideal one means a decrease of the Strehl ratio. However, it can be eliminated by further optimizing process parameters such as flood exposure dosage and reflow temperature setting.

The lensing effect of the fabricated microlens array was tested as well. Fig. 7(a) shows the testing setup, in which a pattern displayed by a mobile phone screen was adopted as the object. In this case, the microlens array was placed on the phone screen and a glass plate with a thickness of about 1.6 cm was inserted between them to control the object distance. The image of the object formed by the microlenses was then captured by a microscope. As is shown in Fig. 7(b), the captured image is quite clear, which indicates a good imaging performance of the fabricated microlens.

It's worth pointing out that, contact angle, which is a material constant depending on interfacial tensions between substrate, photoresist and air, can affect the actual microlens profile significantly.[12] Therefore, one can also use different combinations of photoresist (novolak/diazo type) and substrate to obtain optimal reflow results. The method we demonstrated in this work is compatible with other available approaches to improve the focal number of the microlens such as using a base layer, pre-shaped photoresist patterns, *etc.*

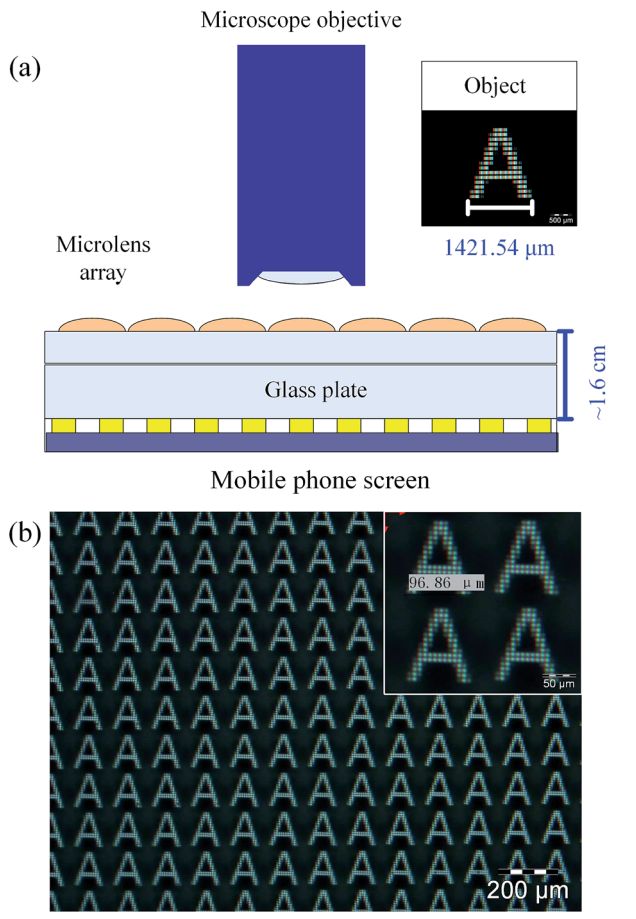

Fig. 7 Imaging test of the fabricated microlens array: (a) configuration of the test setup, (b) images of the object formed by the microlenses.

Conclusions

In conclusion, a novel thermal reflow method is proposed and demonstrated in this work to produce microlenses with enlarged $F^{\#}$. It is found that final profile of the microlens can be controllably tuned by adjusting the flood exposure dosage and using an upside-down reflow configuration. Moreover, in combination with other available approaches, it should be possible to achieve the microlenses with an even higher focal number.

Acknowledgements

The authors acknowledge the funding from Natural Science Foundation of China under grant numbers 61475156 and 61361166004. Financial support from Science and Technology Department of Jilin Province under grant no. 20140519002JH is acknowledged as well.

Notes and references

1 P. Nussbaum, R. Völkel, H. P. Herzig, M. Eisner and S. Haselbeck, *Pure Appl. Opt.*, 1997, **6**, 617–636.
2 L. Erdmann and K. J. Gabriel, *Appl. Opt.*, 2001, **40**, 5592–5599.
3 E. Roy, B. Voisin, J. F. Gravel, R. Peytavi, D. Boudreau and T. Veres, *Microelectron. Eng.*, 2009, **86**, 2255–2261.
4 P. S. Salter and M. J. Booth, *Opt. Lett.*, 2011, **36**, 2302–2304.
5 J. Shao, Y. Ding, H. Zhai, B. Hu, X. Li and H. Tian, *Opt. Lett.*, 2013, **38**, 3044–3046.
6 Z. Zang, X. Tang, X. Liu, X. Lei and W. Chen, *Appl. Opt.*, 2014, **53**, 7868–7871.
7 V. K. Shinoj, V. M. Murukeshan, S. B. Tor, N. H. Loh and S. W. Lye, *Appl. Opt.*, 2014, **53**, 1083–1088.

8 D. Xie, X. Chang, X. Shu, Y. Wang, H. Ding and Y. Liu, *Opt. Express*, 2015, **23**, 5154–5166.
9 G. Y. Yoon, T. Jitsuno, M. Nakatsuka and S. Nakai, *Appl. Opt.*, 1996, **35**, 188–192.
10 Z. D. Popovic, R. A. Sprague and G. A. Neville Connell, *Appl. Opt.*, 1988, **27**, 1281–1284.
11 F. T. O'Neill and J. T. Sheridan, *Optik*, 2002, **113**, 391–404.
12 D. Daly, R. F. Stevens, M. C. Hutley and N. Davies, *Meas. Sci. Technol.*, 1990, **1**, 759–766.
13 S. Haselbeck, H. Schreiber, J. Schwider and N. Streibl, *Opt. Eng.*, 1993, **32**, 1322–1324.
14 M. K. Wei, I. Su, M. C. Jung and K. W. Huang, *Tamkang Journal of Science and Engineering*, 2004, **7**, 81–86.
15 S. Audran, B. Faure, B. Mortini, C. Aumont, R. Tiron, C. Zinck, Y. Sanchez, C. Fellous, J. Regolini, J. P. Reynard and G. Hadziioannou, *Proc. SPIE*, 2006, 6153.
16 S. Audran, B. Mortini, B. Faure and G. Schlatter, *J. Micromech. Microeng.*, 2010, **20**, 1–9.
17 T. R. Jay and M. B. Stern, *Opt. Eng.*, 1994, **33**, 3552–3555.
18 Q. Xu, L. M. Yang, X. W. Hu and G. G. Yang, *Acta Opt. Sin.*, 1998, **18**, 1128–1133, in Chinese.
19 Z. B. Ren and Z. W. Lu, *J. Optoelectron., Laser*, 2005, **16**, 150–154, in Chinese.
20 S. Di and R. X. Du, *Proc. SPIE*, 2006, 73811.
21 R. Allen, M. Foster and Y. T. Yen, *J. Electrochem. Soc.*, 1982, **129**, 1379–1381.
22 A. Schilling, R. Merz, C. Ossmann and H. P. Herzig, *Opt. Eng.*, 2000, **39**, 2171–2176.
23 E. B. Dussan V, *Annu. Rev. Fluid Mech.*, 1979, **11**, 371–400.
24 M. Ashraf, C. Gupta, F. Chollet, S. V. Springham and R. S. Rawat, *Optic. Laser Eng.*, 2008, **46**, 711–720.
25 D. W. Jonson, *Proc. SPIE*, 1984, **469**, 72–79.
26 A. Schiltz, P. Abraham and E. Dechenaux, *J. Electrochem. Soc.*, 1987, **134**, 190–194.